9 November 2001

Chemical Physics Letters 348 (2001) 187–193

CHEMICAL PHYSICS LETTERS

www.elsevier.com/locate/cplett

Anomalous potential barrier of double-wall carbon nanotube

R. Saito [a,*], R. Matsuo [a], T. Kimura [a], G. Dresselhaus [b], M.S. Dresselhaus [c]

[a] *Department of Electronic Engineering, University of Electro-Communications, Chofu, Tokyo 182-8585, Japan*
[b] *Francis Bitter Magnet Laboratory, Massachusetts Institute of Technology, Cambridge, MA 02139-4307, USA*
[c] *Department of Physics and Department of Electrical Engineering and Computer Science, Massachusetts Institute of Technology, Cambridge, MA 02139-4307, USA*

Received 21 August 2001; in final form 18 September 2001

Abstract

The stable structure of a double-wall carbon nanotube (DWNT) is calculated for various chirality pairs, $(n,m)-(n',m')$, of inner and outer constituent layers. The stability of a double-wall nanotube is found not to depend on chirality, but rather on the diameter difference between inner and outer layers. However, the potential barrier for the relative displacement of the inner and outer nanotube layers is found to depend significantly on the chirality difference of the pair. Mechanical motions like a bolt–nut pair or discrete rotations can be expected for special pairs of chiralities in double-wall nanotubes, and these special motions will be important for nano-technology.

1. Introduction

Carbon nanotubes [1] has been of great interest as mechanically strong materials and for nanometer size electronics [2–4]. In multi-wall carbon nanotubes (MWNTs), the interlayer interaction between adjacent layers is sufficiently small compared with the intralayer covalent C–C bonding, so that the sliding motion between the constituent layers is easy if the ends of the MWNTs are open. Recently, fullerene-encapsulated single-wall carbon nanotubes, so called peapod [5] nanotubes have been produced [6–8] in which the fullerenes can enter from the opened end by oxidization [5,9]. Furthermore, from the peapod nanotube, a double-wall carbon nanotube (DWNT) can be produced by electron irradiation [10] or by heating [11] in which only the fullerenes are decomposed into an inner single carbon nanotube shell. Thus a DWNT becomes a new carbon material whose inner nanotube diameter is selected for an outer carbon nanotube of given diameter and chirality. One theoretical interest of this paper is what kind of chirality or diameter of the inner SWNT is stable for a given outer (n,m) pair. Another question is how easy it is to slide inner and outer nanotubes past one another for different pairs of chiralities. In this Letter we show that the sliding motion depends strongly on the chirality pair.

Theoretically, Charlier and Michenaud have calculated the potential barrier of a $(5,5)$–$(10,10)$ DWNT using the local density approximation

* Corresponding author. Fax: 0081-424-43-5210.
E-mail address: rsaito@ee.uec.ac.jp (R. Saito).

0009-2614/01/$ - see front matter
PII: S0009-2614(01)01127-7

(LDA), in which the potential barrier per carbon atom for sliding motion is anisotropic. The calculated energy barriers were found to be 0.52 and 0.23 meV/atom, respectively, in the directions along and circumferential to the nanotube axis [12]. Palser calculated the barriers of a $(5,5)$–$(10,10)$ DWNT also, using a tight-binding method, and got 0.295 and 0.085 meV/atom in the directions along and circumferential to the nanotube axis, respectively [13]. Although the calculated barrier values are different, these two calculations show that the sliding of nanotube layers past one another is relatively easy along the nanotube axis direction. However, these calculations are only for armchair–armchair double-wall nanotubes which are commensurate between the inner and outer layers. The general structure of double-layer carbon nanotubes is *incommensurate* and the constituent layers are generally *chiral*. Kolmogorov and Crespi calculated the corrugation as a function of carbon atoms for several chirality pairs, and found the corrugation to become anomalously small ($\sim$0.1 meV/atom) for incommensurate structures between the inner and outer layers [14]. Roche et al. [15] reported that the incommensurability in MWNTs may give unconventional electronic conduction mechanism. Here we calculate the interlayer potential energy systematically for many chirality pairs.

The X-ray diffraction patterns of MWNTs show an average interlayer distance of $c = 3.44$ Å, consistent with the turbostratic layer stacking of graphene layers in MWNTs, but larger than $c = 3.35$ Å for graphite [16] with the AB Bernal stacking. In the incommensurate case, the sliding motion of the adjacent layers does not always go along the circumferential or nonotube-axis directions. Thus it is expected that the direction for the relative movement of the constituent layers is spiral, with a spiral angle that depends on the pair of chiralities. The calculated potential shapes are in fact spiral, whose direction of sliding motion depends strongly on the relative chiralities.

The interlayer interaction between graphene layers has been discussed for graphite AB stacking [17], a C_{60} crystal [18], multi-wall fullerenes [19], and C_{60} on graphite [20] for which the electronic interaction between π bonds in the different layers is not negligible, but has values in the 0.30–0.40 eV range. These values are estimated from the γ_1, γ_3, and γ_4 tight-binding parameters [21] that characterize the Slonczewski–Weiss Hamiltonian [22]. The γ_1, γ_3, and γ_4 parameters represents, respectively, the C–C interaction between A–A, A–B, and B–B carbon atoms of the AB Bernel stacking of graphite. In AB stacking, A represents carbon atoms which have another A carbon atom in the nearest neighbor layers at $(0,0,\pm c)$, while the corresponding positions of $(0,0,\pm c)$ from the B atom are empty at the center of the hexagonal ring in the nearest neighbor layers. However, the wavefunction of the π atomic orbital is delocalized over a relatively large distance, compared with the in-plane C–C bond length, and the total energy variation per carbon atom associated with sliding a graphene plane is much smaller than the γ_i $(i = 1,3,4)$ parameters.

2. Method

Here we simply adopt the 6–12 van der Waals (vdW) potential $V(r) = 4\epsilon\{-(\sigma/r)^6 + (\sigma/r)^{12}\}$ with $\epsilon = 2.968$ meV and $\sigma = 3.407$ Å for the interlayer interaction which reproduces the layer distance of 3.354 Å and the elastic constant $C_{33} = 4.08$ GPa of graphite [18,23]. The upper and lower cutoff distances for calculating the vdW interaction are 2.1 and 17.5 Å, respectively. The upper cutoff is determined such that the interlayer distance, 3.354 Å, is reproduced for three-dimensional graphite. In fact, the length, 17.5 Å, corresponds to five layers of graphite. The interlayer distance decreases monotonically from 3.407 to 3.354 Å, by increasing the number of layers from one to five layers for this cutoff. In order to avoid a discontinuity of the potential value at the cutoff, which might affect the optimization, the vdW value is smoothly connected to zero by a sine function between the lengths of 2.0 and 2.2 Å, and between 16.5 and 17.5 Å. It is very efficient to use the vdW interaction for making calculations for many different DWNTs. It should be mentioned that the calculated potential depth cannot be evaluated quantitatively. However, the shape of the potential can be shown to be correct.

The atomic coordinates of carbon atoms in each constituent layer are optimized using the Tersoff potential [24]. The upper cutoff of the Tersoff potential is given by 1.95 Å, and we connect the potential value smoothly to zero by a sine function between 1.8 and 2.1 Å. Since the energy scale of the Tersoff potential is three orders of magnitude larger than the vdW potential, the modification of the C–C bond lengths by the vdW interaction can be neglected as a first approximation. The Tersoff potential reproduces the sp, sp^2 and sp^3 covalent bonding with the same function of the potential, but the optimized values of periodic graphite (1.467 Å) and diamond (1.548 Å) are slightly larger than the observed values of 1.421 and 1.544 Å [24]. This is because the potential parameters of the Tersoff potential are fitted to the LDA calculation of sp^3 covalent bonding. To avoid any difference between the calculated and experimental sp^2 bond length of carbon nanotubes, we artificially introduce a scaling parameter 0.9685 for all optimized coordinates. This factor is close to that proposed for the C_{60} system, 0.963, by Okada [25], which is reasonable, since the averaged bond length of a nanotube is larger than that for graphite and smaller than the pentagonal ring of a C_{60} molecule. Since there is no overlap of the vdW and Tersoff potentials as a function of the two-atom C–C distance, we can treat the optimization problems separately.

The optimization method used to get the atomic coordinates is the so-called molecular dynamics method (MDM) in which we first give a random velocity to each atom and then cool the system to get the optimized positions. In the MDM, we take a time step of 2.5 fs and a cooling rate for the velocity of 0.9 per time step, with which we can get an optimized structure within 100 steps. This corresponds to an artificially, rapid cooling rate. However, we found that we get a reproducible value after several minutes for the locations of 1000 carbon atoms using a UNIX workstation. For comparison, we made a computer program using the conjugated gradient (CG) method for optimization, too, but we found that the CG method is not as efficient as the MDM approach for long carbon nanotubes with ends. In fact, if the initial coordinates have equal C–C bond lengths, no forces act on the carbon atoms except for the edge atoms. Thus, it takes a lot of time to correct the bond lengths from the edge to the middle region of a nanotube. Both programs were written by ourselves and they are $O(N)$ programs in which the computational time is proportional to the number of atoms, N.

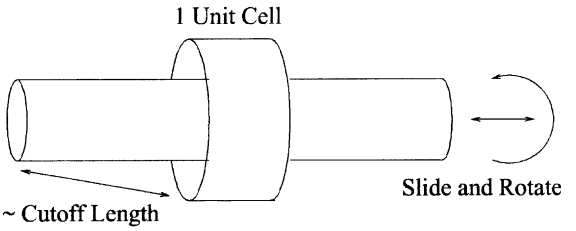

Fig. 1. The DWNT structure used in the calculation. In order to neglect the edge–edge interaction, the distance between the inner and outer edges is taken to be larger than the cutoff length 17.5 Å. The length of the inner tube is taken to be more than one unit cell of the outer tube and larger than 24.0 Å.

In Fig. 1 we show a double layers system of MWNTs adopted to the present calculation. Since the outer and inner nanotubes are generally incommensurate in the direction of the nanotube axis, we cannot define a unit cell for a general DWNT. Thus, we need to consider the finite length of the DWNT. In this case, one of the two nanotubes should be much smaller than the other, so that the overlapping area for the inner and outer nanotubes does not change as a result of the relative motion of the tubes. The lengths of the outer and inner tubes are taken to be more than 24 and 140 Å, respectively. The length of the shorter, outer nanotube is chosen so that the effect of the edge of the outer nanotube does not contribute much to the total adiabatic potential, which is checked by changing the length of the outer tube. The length of the longer, inner nanotube is chosen so that the potential range of the vdW interaction is shorter than this length.

3. Calculated results

In Fig. 2, we plot the potential energy per carbon atom of the vdW potential for the optimized structure of a DWNT as a function of the inter-

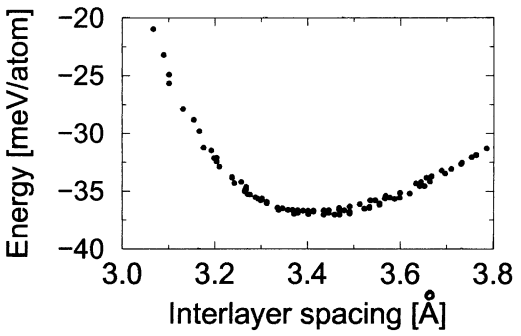

Fig. 2. The potential energy of the vdW potential per carbon atom plotted as a function of the interlayer spacing between the inner and outer layers of the DWNT in the unit of Å. Each dot in the figure corresponds to a pair of $(n,m)-(n',m')$ DWNTs.

layer spacing between the inner and outer layers. Each dot in the figure corresponds to a pair of $(n,m)-(n',m')$ DWNTs. We take a random sampling of pairs for which the diameter of the outer layer is less than 2 nm. It is clear from Fig. 2 that the stability of a DWNT depends only on the interlayer spacing and has a minimum around 3.4 Å. The stable potential is almost flat for interlayer spacings from 3.3 to 3.5 Å. Since there are a number of $(n,m)-(n',m')$ pairs in the flat region of the graph, we do not have a stable pair of chiralities for DWNTs. One reason why the stable potential energy does not depend on the chirality pairs is the fact that the vdW potential smoothly changes as a function of distance compared with the C–C bond length. As a result, the geometry differences due to the various chirality pairs are smeared out with regard to their total energy values. It is pointed out that the intralayer C–C bond length is not changed by the interlayer interaction because of the three orders of magnitude difference in their potential values. The absence of a stable pair of DWNTs might be good news telling us that we can synthesize any pairs of DWNTs, such as metal–metal, metal–semiconducting, or semiconducting–semiconducting nanotubes. In fact, Raman spectra show many possible radial breathing mode frequencies for individual SWNTs [11]. This result can be tested experimentally by extending single-nanotube Raman spectroscopy [26] so that we can assign (n,m) values to the constituent layers.

In Fig. 3 we show the results for the adiabatic potential of a $(6,4)$–$(16,4)$ DWNT for the movement of the outer layer relative to the inner layer. The two degrees of freedom of motion are taken to be sliding along the nanotube axis and rotation around the nanotube axis, which correspond to the vertical and horizontal axes of the figure, respectively. The darker area corresponds to the more stable area. In Fig. 3 we select (a) one and (b) two unit cells for the outer $(16,4)$ nanotube. It is clear that there is no difference in the potential energy in (a) and (b) in units of eV

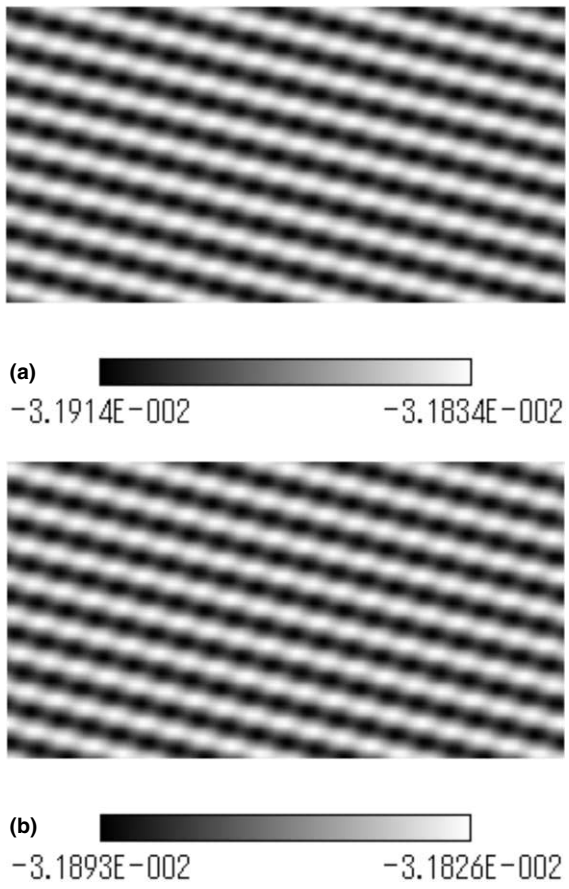

Fig. 3. The potential shape of a $(6,4)$–$(16,4)$ DWNT, with an outer nanotube having a length of (a) one and (b) two unit cells. The vertical and horizontal directions correspond to the sliding direction along the nanotube axis and the circumferential direction, respectively. The maximum and minimum potentials of the gray scale that are given for each DWNT determines its ΔE value in the unit of eV/atom.

per carbon atom, showing that this adiabatic potential does not come from the edge effect but rather comes from the interlayer effect. It is noted that the origin of the potential is not the same between (a) and (b) and that the difference of the phase of potential cannot be discussed. The difference between the potential values in (a) and (b) is of the order of 0.01 meV/atom. When the number of atoms in the outer layer are on the order of 10 000, we can expect a large potential barrier of 1 eV per tube if all the atoms moves in the same way.

The potential shapes exhibit many patterns, as shown in Fig. 3. When we pull on the outer (or inner) nanotube, the nanotube can screw or slide with rotation. In Fig. 4 we show several examples of the adiabatic potential whose shape is determined by the $(n,m)-(n',m')$ pairs. The spiral angle for easy movement can be changed form 0° to 90°, as shown for the two DWNTs in (a) $(9,0)$–$(18,0)$ and (b) $(5,5)$–$(10,10)$. In particular, the easy direction for $(5,5)$–$(10,10)$ is consistent with previous results [12,13] though the barrier height of the present work has much smaller values, 0.025 and 0.008 meV/atom along the circumferential and nanotube axis directions, respectively. It is simply because the adopted vdW potential has smaller values than the previous ones. Moreover, as shown in the case of (c) $(8,-2)$–$(14,5)$, the potential *minimum* can be localized as a dot. In this case we can expect a discrete (ratchet) motion for the DWNT. In the case of (d) $(9,0)$–$(15,4)$, on the other hand, the potential *maximum* is localized. A variety of potential shapes, such as a nano-bolt–nut pair like those shown in (e) and (f), will be useful for specific mechanical applications.

Calculation of the potential pattern for a given $(n,m)-(n',m')$ pair is not trivial and therefore no general formula is given in this paper for the potential pattern. If there should be experimental evidence for such effects [27] in the future, we should then consider the development of an appropriate formula. Trivial results are obtained when both inner and outer nanotubes are either armchair or zigzag nanotubes. Since armchair and zigzag nanotubes have a common mirror plane along the nanotube axis, the potential shape is either parallel or perpendicular to the nanotube axis. In armchair–armchair DWNTs, the nanotube axis direction is an easy direction of movement, while for zigzag–armchair or zigzag–zigzag DWNTs, the circumferential direction is an easy direction. For general chiral nanotube pairs, the potential shape exhibits a stripe pat-

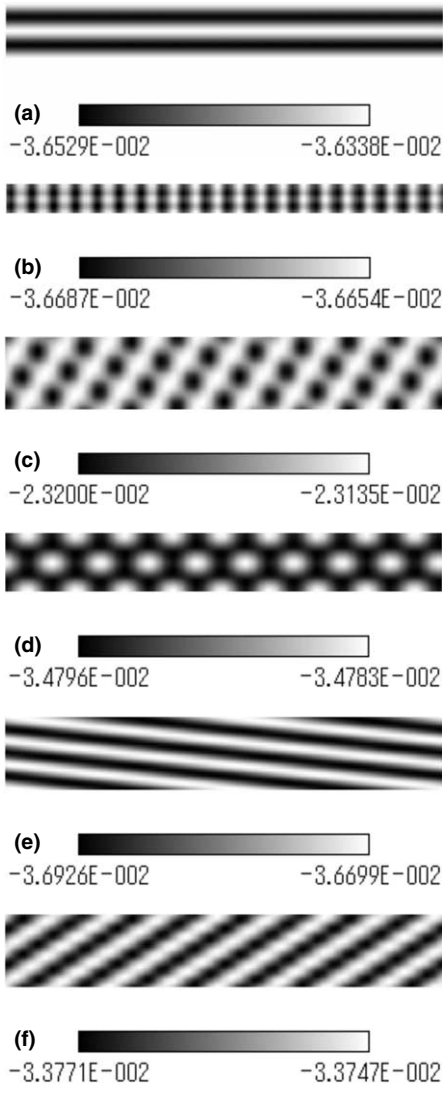

Fig. 4. The potentials shapes of (a) $(9,0)$–$(18,0)$, (b) $(5,5)$–$(10,10)$, (c) $(8,-2)$–$(14,5)$, (d) $(9,0)$–$(15,4)$, and (e) $(8,2)$–$(17,2)$ (f) $(8,2)$–$(12,8)$ DWNTs. The maximum and minimum potentials of the gray scale that are given for each DWNT determines its ΔE value in the unit of eV/atom.

terns as shown in (e) $(8,20)$–$(17,2)$ and (f) $(8,2)$–$(12,8)$, whose spiral angles can be seen to be controlled by changing the chiralities of the pair.

Another important point is that most of chirality pairs have a negligibly small potential difference ΔE (1–10 μeV/atom), between their potential maxima and minima, because of their incommensurate structure. In an incommensurate lattice structure, many atoms are in different potential positions, and their average potential does not change much as a result of the movement. For example, for the inner $(6,4)$ nanotube, $(16,2)$, $(14,5)$, $(10,10)$, $(16,4)$ are outer nanotubes for which ΔE is relatively large compared with that for other possible outer (n,m) nanotubes. For the $(5,5)$ inner nanotube, the $(14,5)$, $(15,5)$, $(10,10)$ outer nanotubes show large ΔE values, while for the $(9,0)$ inner nanotube, the $(14,5)$ and $(18,0)$ outer nanotubes show large ΔE values. Since the ratio of the diameters for the inner and outer nanotubes is close to 1:2 in this case, $(5,5)$–$(10,10)$ and $(9,0)$–$(18,0)$ are reasonable pairs for getting a large ΔE. However, it is not clear why $(14,5)$ is a special outer nanotube which gives a large ΔE is conjunction with the $(5,5)$ inner nanotube. The calculated results show that ΔE does not depend on the interlayer distance and large ΔE values are completely due to a chirality effect on the mechanical motion.

4. Conclusion

We have examined the optimized geometry and adiabatic potential of a DWNT for a variety of sets of inner and outer nanotube chiralities. Although the optimized stable energy clearly depends on the interlayer distance between the inner and outer nanotube layers, the adiabatic potential height depends much more sensitively on the chirality pair and not so much on the interlayer distance. The potential shape can be a spiral stripe, a local minimum array, or a local maximum array. If some experimental technique [27] can be found to observe the predicted anomalous behaviors, control of the chirality pairs of DWNTs could be interesting for applications to nano-mechanics.

Acknowledgements

R.S. acknowledges a Grant-in-Aid (No. 13440091) from the Ministry of Education, Japan. The MIT authors acknowledge support under NSF Grants DMR 01-16042, INT 98-15744, and INT 00-00408.

References

[1] S. Iijima, Nature 354 (1991) 56.
[2] M.S. Dresselhaus, G. Dresselhaus, P.C. Eklund, Science of Fullerenes and Carbon Nanotubes, Academic Press, New York, NY, 1996.
[3] R. Saito, G. Dresselhaus, M.S. Dresselhaus, Physical Properties of Carbon Nanotubes, Imperial College Press, London, 1998.
[4] M.S. Dresselhaus, G. Dresselhaus, Ph. Avouris, in: Carbon Nanotubes: Synthesis, Structure, Properties and Applications, Springer Series in Topics in Appl. Phys., vol. 80, Springer, Berlin, 2001.
[5] Y. Zhang, S. Iijima, Z. Shi, Z. Gu, Philos. Mag. Lett. 79 (1999) 473.
[6] B.W. Smith, M. Monthioux, D.E. Luzzi, Nature 396 (1998) 323.
[7] B.W. Smith, D.E. Luzzi, Chem. Phys. Lett. 321 (2000) 169.
[8] K. Hirahara, K. Suenaga, S. Bandow, H. Kato, T. Okazaki, H. Shinohara, S. Iijima, Phys. Rev. Lett. 85 (2000) 5384.
[9] H. Kataura, Y. Kumazawa, N. Kojima, Y. Maniwa, I. Umezu, S. Masubuchi, S. Kazama, Y. Ohtsuka, S. Suzuki, Y. Achiba, Mol. Cryst. Liq. Cryst. 340 (2000) 757.
[10] J. Sloan, R.E. Dunin-Borkowski, J.L. Hutchison, K.S. Coleman, V.C. Williams, J.B. Claridge, A.P.E. York, C. Xu, S.R. Bailey, G. Brown, S. Friedrichs, M.L.H. Green, Chem. Phys. Lett. 316 (2000) 191.
[11] S. Bandow, M. Takizawa, K. Hirahara, M. Yudasaka, S. Iijima, Chem. Phys. Lett. 337 (2001) 48.
[12] J.-C. Charlier, J.P. Michenaud, Phys. Rev. Lett. 70 (1993) 1858.
[13] A.H.R. Palser, Phys. Chem. Chem. Phys. 1 (1999) 4459.
[14] A.N. Kolmogorov, V.H. Crespi, Phys. Rev. Lett. 85 (2000) 4727.
[15] S. Roche, F. Triiozon, A. Rubio, D. Mayor, Phys. Lett. A 285 (2001) 94.
[16] Y. Saito, T. Yoshikawa, M. Inagaki, M. Tomita, T. Hayashi, Chem. Phys. Lett. 204 (1993) 277.
[17] K. Yoshizawa, T. Kato, T. Yamabe, J. Chem. Phys. 105 (1996) 2099.
[18] J.P. Lu, X.P. Li, R.M. Martin, Phys. Rev. Lett. 68 (1992) 1551.
[19] J.P. Lu, Phys. Rev. B 49 (1994) 5687.
[20] S.N. Song, X.K. Wang, R.P.H. Chang, J.B. Ketterson, Phys. Rev. Lett. 72 (1994) 697.

[21] R. Saito, H. Kamimura, Phys. Rev. B 33 (1986) 7218.
[22] J.C. Slonczewski, P.R. Weiss, Phys. Rev. 109 (1957) 272.
[23] O.L. Blakslee, D.G. Proctor, E.J. Seldin, G.B. Spence, T. Weng, J. Appl. Phys. 41 (1977) 3373.
[24] J. Tersoff, Phys. Rev. Lett. 61 (1988) 2879.
[25] S. Okada, Thesis, Tokyo Institute of Technology, Tokyo, 1986.
[26] A. Jorio, R. Saito, J.H. Hafner, C.M. Lieber, M. Hunter, T. McClure, G. Dresselhaus, M.S. Dresselhaus, Phys. Rev. Lett. 86 (2001) 1118.
[27] J. Cumings, A. Zettl, Science 289 (2000) 602.